*Proceedings of the 11th Brazilian Congress of Thermal Sciences and Engineering -- ENCIT 2006*
*Braz. Soc. of Mechanical Sciences and Engineering -- ABCM, Curitiba, Brazil,- Dec. 5-8, 2006*

**Paper CIT06-0740**

# ASPECTS OF ISOLATED NACELLES NEAR THE GROUND DURING CROSSWIND OPERATION

**Luís Gustavo Trapp**
Empresa Brasileira de Aeronáutica S.A. – EMBRAER
Av. Brigadeiro Faria Lima, 2170
12227-901 São José dos Campos - SP
email: Gustavo.Trapp@embraer.com.br

**Henrique Gustavo Argentieri**
Empresa Brasileira de Aeronáutica S.A. – EMBRAER
Av. Brigadeiro Faria Lima, 2170
12227-901 São José dos Campos - SP
email: Henrique.Argentieri@embraer.com.br

**Francisco José de Souza**
Empresa Brasileira de Aeronáutica S.A. – EMBRAER
Av. Brigadeiro Faria Lima, 2170
12227-901 São José dos Campos - SP
email: Francisco.Souza@embraer.com.br

**Roberto da Motta Girardi**
Instituto Tecnológico da Aeronáutica - ITA
Praça Marechal Eduardo Gomes, 50
2228-900 – São José dos Campos – SP
email: Girardi@ita.br

***Jet aircraft operation on the ground is affected by wind and the aircraft engines are particularly affected by crosswinds and tailwinds. Some aspects of the crosswind operation are the inlet sepation and the vortex that forms between the engine inlet and ground at very low to zero aircraft speeds. This ground vortex is created by the interaction between the inlet flow and the crosswind, can suck foreign objects into the engine and damage it and also affect engine operability. Ground vortices have been widely studied since the 1950s, more recently CFD tools have been applied to their understanding with relative success. The present study analyze some aspects of the nacelle operation with crosswinds near the ground, involving the inlet ground vortex and its visualization and some factors that influence vortex strength and inlet lip separation.***

*Keywords: propulsion, CFD, crosswind, operability, engine, nacelle, visualization techniques, post-processing*

## 1. Introduction

Aircraft operation on the ground can be adversely impacted by wind, particularly when the wind is not frontal. Crosswind impacts all aspects of an aircraft ground operation: start, taxiing, takeoff and landing. Aircraft start is mainly affected by tailwind because it may drive the engine rotors to rotate opposite to its normal direction, however if the winds are too great it is always possible to reorient the aircraft with its nose into the wind before starting the engines. Crosswind affects taxiing in a lesser way: aircraft lift and speed are not great, engine speed is also low therefore the aircraft is usually controllable by the nose steering; engine behavior is normally not much affected by crosswinds at low engine speeds. Crosswind landings can affect the aircraft during approaches by wandering it off to the runway side, by leading it to asymmetric touchdowns and by the weather vaning effect after touch down and thrust reverser operation.

During crosswind takeoffs the aircraft has a weather vaning tendency and controllability may be difficult during initial phases of takeoff due to low vertical tail efficiency at low speed. It is during takeoffs that crosswind has a greater effect on the engine, mainly when the aircraft is static at the runway threshold at high power, just before brake release and the takeoff roll.

A high power static engine is affected by crosswind in at least three different ways: fuselage vortex shedding, inlet separation and ground vortex. These phenomena generate a non-uniform flow for the inlet that affects the engine operation and may even affect its physical integrity. This non-uniform flow ingested by the inlet is generally referred to as “inlet distortion” or more simply “distortion”.

Effects of distortion on the engine have been studied extensively and aircraft and engine manufacturers are able to assess its effects on fan blade vibratory stresses through standard procedures (SAE, 1999). However most of the research has been made to correctly simulate flight conditions distortion on test benches and isolated inlets (Beale et alii, 2002).

Engine operation on the ground induces inlet flow far below sonic values, however if crosswind exists the flow speed on the inlet internal surface can become locally supersonic (Boles and Stockmann, 1979) and induce inlet separation, which is a major source of inlet distortion.

Another issue raised on crosswind operation is the vortex that forms between the engine inlet and ground at very low to zero aircraft speeds. This ground vortex, created by the interaction between the inlet flow and the crosswind, can suck foreign objects into the engine and damage it, also affecting engine operability.

According to Yadlin and Shmilovich, 2006, the angular momentum due to the turning of the flow into the engine inlet in combination with the stagnation streamline off the ground plane leads to the creation of the ground vortex, in a mechanism that can be usually considered as an inviscid phenomenon.

CFD tools have been applied recently to the understanding of the ground vortex with relative success. Nakayama and Jones, 1999, used panel methods to simulate the inlet and ground interaction, noting that the wind speed needed to blow the vortex away was lower than the measured experimentally; Navier-Stokes calculations, on the other hand, were beyond the available computational capability at the time due to the refined grid needed to capture the vortex. Tourette, 2002, performed N-S analysis of an isolated nacelle near the ground with different turbulence models and was able to get a good comparison of static pressure over the nacelle lip with experimental results, however fan face inlet distortion, vortex intensity and location were less accurate. Yadlin and Shmilovich, 2006, performed CFD N-S analysis of installed nacelles on a high wing aircraft, also taking into account the effect of the thrust-reverser.

The present study analyze some aspects of the nacelle operation with crosswinds near the ground, involving the inlet ground vortex and its visualization and some factors that influence vortex strength and inlet lip separation.

## 2. Test case

In order to study the inlet vortex interaction with the ground it was chosen to use the DLR F6 nacelle (DLR, 2003), a wind tunnel model long duct nacelle from the wing-body-pylon-nacelle configuration used on the AIAA Drag Prediction Workshops. This nacelle has a publicly available lofting and is originally a through-flow nacelle (TFN), it was modified to better represent a real engine, incorporating outlet and inlet boundary conditions (Figure 1).

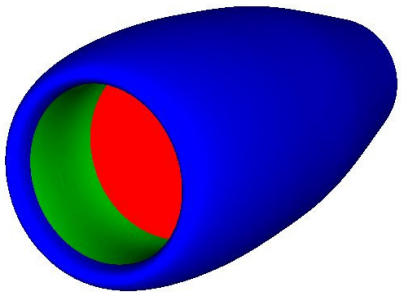

Figure 1 – DLR F6 long duct nacelle

Geometrical parameters of the DLR-F6 nacelle are given on Table 1

Table 1 – DLR-F6 nacelle dimensions

| | Dimension (mm) |
|---|---|
| Length | 180.0 |
| Hilite Diameter | 55.1 |
| Inlet Throat Diameter | 49.4 |
| Fan Diameter | 54.8 |
| Max Diameter | 76.2 |
| Exhaust Diameter | 50.0 |

Major inlet parameters that impact engine operation are the inlet diffuser ratio and the inlet contraction ratio. The inlet diffusion ratio is the ratio between the fan diameter and the inlet throat; it influences the flow speed that the fan will operate. The diffusion ratio will also impact the inlet length because the expansion shall be smooth enough to avoid separation. The inlet contraction ratio is defined as the ratio between the inlet hilite and the inlet throat areas and dictates the nacelle flexibility to ingest flows that are not aligned with its inlet (i.e. flight at high angles of attack, sideslips, crosswind operation on the ground, etc.). This DLR-F6 nacelle design parameters are given on Table 2.

Table 2 – DLR-F6 nacelle design parameters

| | |
|---|---|
| Diffusion ratio | 1.1 |
| Contraction ratio | 1.24 |

Boles and Stockmann, 1979, have determined that inlet peak Mach numbers between 1.4 and 1.6 induce separation and these are a direct function of the inlet contraction ratio, the lower the contraction ratio the greater the chance of separation when the flow is misaligned with the inlet. However a high contraction ratio inlet, despite its benign crosswind characteristics, has, at cruise operation, higher spillage, which increases external drag – therefore the contraction ratio has to be balanced to fulfill both ground and cruise requirements.

Other factors that influence the inlet lip Mach number during aircraft ground operation are the inlet mass flow (function of engine thrust setting), wind speed and wind direction relative to the inlet.

In order to assess the behavior of the nacelle near the ground a typical condition was set: sea level, aircraft static, ISA day, 90° crosswind and fan face with 90 000 Pa absolute static pressure. Crosswind effects were evaluated between 5 and 30 knots speeds (between 2.6 and 15.4 m/s). The nacelle was positioned at a distance between hilite (i.e. the leading edge of the nacelle) and the ground equal to the hilite radius.

It is important for the engine that the nacelle operates in crosswind conditions without flow separation. The DLR F6 nacelle was designed for cruise analysis and does not have a contraction ratio compatible with high crosswinds. In order to proceed with the study its contraction ratio was modified to a 1.34 ratio to make it more resistant to high crosswind levels, keeping all other geometrical parameters the same. The new nacelle was designated DLR F6 MOD1.

## 3. Numerical setup

The compressible, three-dimensional Navier-Stokes equations were solved by the commercial code CFD++ 5.2. For the turbulence modeling, a RANS (Reynolds-Averaged Navier-Stokes) approach was adopted, and the realizable k-epsilon model was employed. Advanced wall functions available in CFD++ were used at all wall surfaces. A hybrid tetrahedra-prism mesh was generated with the commercial code ICEM 10.0 for the viscous runs, while a simpler tetrahedral mesh was used on the Euler initial runs. The grids for the isolated nacelle contained nearly 5 million elements in the hybrid case and 3 million in the tetrahedral case. The parameter y+, which is important in evaluating the ability of the grid to capture near-wall effects, was below 10 in all viscous cases.

## 4. CFD Results

### 4.1. Vortex visualization

The inlet vortex is a low pressure, high vorticity, high speed flow that is ingested by the engine inlet. However the physical phenomenon around a static inlet near ground is more complex than only a vortex: high levels of vorticity are generated by the wind on all walls, vortex shedding is triggered leeward of the nacelle and low pressure is generated inside the engine inlet by the engine. Therefore it is difficult to isolate the ground vortex from the other phenomena.

A major issue during the CFD results post-processing was to define a methodology to correctly capture and isolate the ground vortex. Different post-processing criteria were evaluated and are presented in this section. Some criteria simply deal with the basic scalar results; other methods involve operations with the vectors, while some work also with the geometrical cell characteristics.

On the vortex core there is a low pressure region and an obvious post-processing choice is to detect the vortex with a static pressure isosurface. Figure 2 shows CFD results of a 20 knots crosswind upon the nacelle through a pressure isosurface of 99 500 Pa. The vortex boundaries near the ground can be seen, however as the vortex approaches the inlet the negative pressure is increased due to engine suction and hid the vortex, making this kind of post processing unsuitable for vortex tracking. Also in figure 2 the ground is colored by static pressure intensity, the center of the vortex can then be seen on the ground.

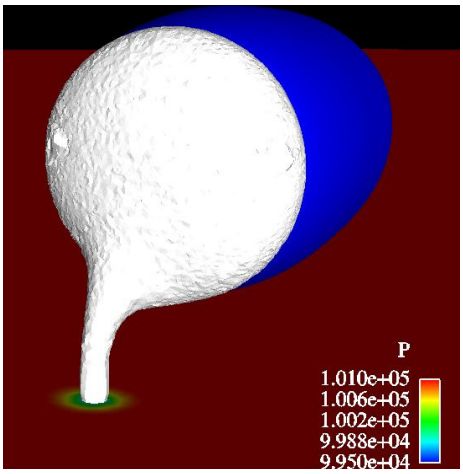


Figure 2 – Isosurface of low pressure near the nacelle inlet

Figure 3 shows the same case and a high vorticity isosurface. Near the walls, as expected, the speeds are higher and therefore more vorticity is created, rough contours of the vortex can be seen in the same location where the pressure isosurface showed it. The inlet region is visible; however the vorticity isosurface does not get far into it, not reaching the fan.

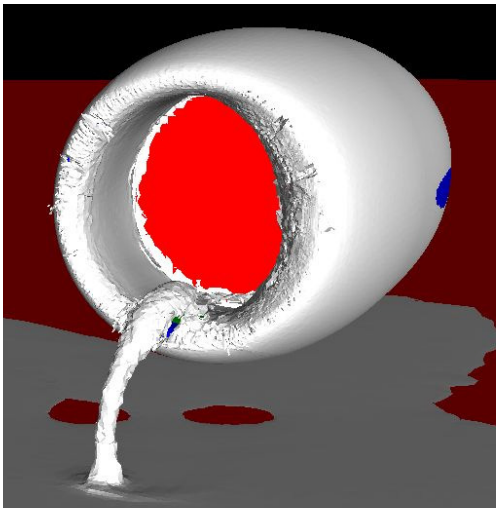

Figure 3 – Isosurface of vorticity near the nacelle inlet

Another choice is to use relative helicity (Ensight, 2005) or normalized helicity (Sadarjoen et alii, 1998) - $h_n$, which is the defined as:

$$h_n = \frac{\vec{v} \cdot \vec{\omega}}{|\vec{v}| \cdot |\vec{\omega}|}$$

Where $\vec{v}$ is the velocity vector and $\vec{\omega}$ the vorticity vector. Relative helicity represents the cosine of the angle between flow velocity and vorticity. Isosurfaces of highest (yellow) and lowest (white) helicity are depicted on figure 4, but do not capture the ground vortex. It seems that while the ground vortex vorticity is high, the resulting flow velocity in the suction direction is not. Therefore, when comparing the ground vortex region to other areas on the domain the vortex is not easily distinguishable.

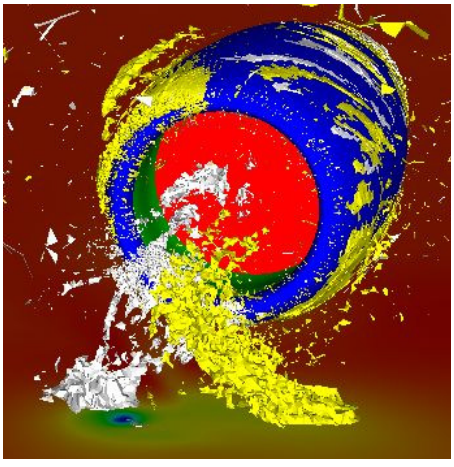

Figure 4 – Isosurfaces of helicity near the nacelle inlet, $h_n$=0.995 (yellow) and $h_n$=-0.995 (white)

The function $\lambda_2$ (Jeong and Hussain, 1995) is defined as the second largest eigenvalue of the tensor $S^2 + \Omega^2$, where $S = \frac{1}{2}(\vec{\nabla}\vec{v} + (\vec{\nabla}\vec{v})^T)$ and $\Omega = \frac{1}{2}(\vec{\nabla}\vec{v} - (\vec{\nabla}\vec{v})^T)$.

Negative results of $\lambda_2$ indicate vortical regions and are shown on Figure 5. They show a approximate location for the vortex, but discontinuous, with spurious regions also selected together with most of the nacelle inlet wall.

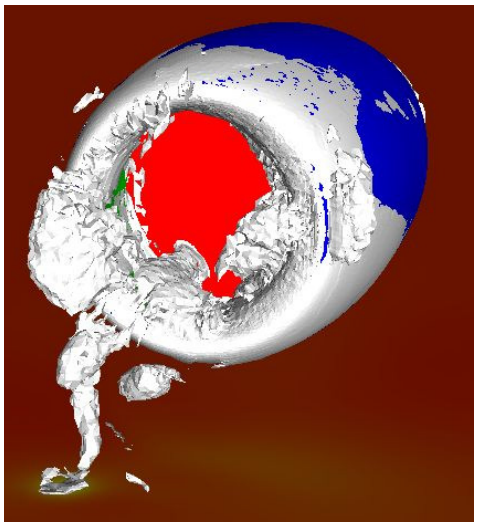

Figure 5. – isosurface of $\lambda_2$ equal $-8.10^5$

The function Q (Jeong and Hussain, 1995) is the second invariant of the velocity gradient tensor $\nabla\vec{v}$ :

$$Q = \tfrac{1}{2}\left( |S|^2 - |\Omega|^2 \right)$$

If the velocity is taken in index notation ($v_{i,j}$) then the function becomes:

$$Q = -\frac{1}{2}\left(v_{i,j}v_{j,i}\right)$$

Regions of Q function positive indicate vortical regions, which are shown on fig. 6. This method shows lots of improvement when compared with the $\lambda_2$ method, showing an almost continuous vortex, but still including the inlet wall region.

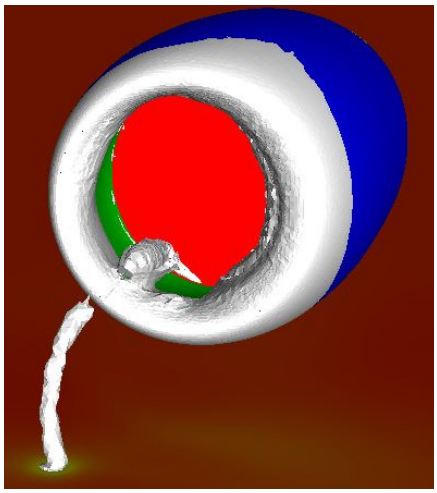

Figure 6 – isosurface of Q equal $10^7$

The vortex cores function from Ensight was then tested (Ensight, 2005). It helps visualize the centers of swirling flow by creating vortex core segments from the velocity gradient tensor of the flow field. Results for vortex core visualization are shown on fig. 7 together with the ground static pressure isosurface.

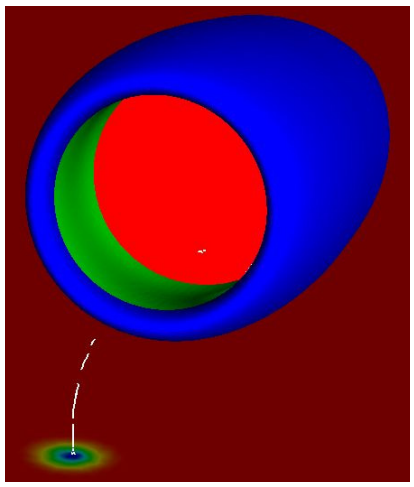

Figure 7 - vortex cores on the engine inlet

The vortex cores showed to be much better on vortex characterization – the ground vortex being much more intense than other vertical phenomena like vortex shedding and wall vorticity. However the vortex core visualization involves some operations that need to be performed within the mesh grid, which is difficult to implementate on a commercial post-processing code, if it does not includes this feature.

The vortex core algorithm also has problems finding cores of curved vortices and usually fails to predict vortex core segments in regions of weak vortices (Ensight, 2005). The latter problem does not impact the ground vortex identification because it is supposed to be the stronger vortex on the system. The curved vortices un-identification seems to be affecting the visualization because the vortex is not captured approximately on the region where it is turning more steeply into the engine. However a turn around to this problem is to release particle traces from the vortex core which will approximately show the vortex path.

### 4.2. Influence of viscosity

Once a approximate method of vortex visualization was defined another aspects of the nacelle operation with crosswinds could be studied, initially with an inviscid fluid.

Initial CFD runs were performed with 30 kts crosswind and showed separation. Also this wind intensity blew the inlet vortex away and avoided it from attaching to the ground. Similar results occurred with a 15 knots crosswind and can be seen on Fig 8, where the nacelle wall and pressure outlet are colored by Mach intensity and vortex cores are depicted on the left of the nacelle. Wall separation is seen in the low Mach number contours on the pressure outlet. The maximum Mach number on the nacelle lip was of the order of 0.80.

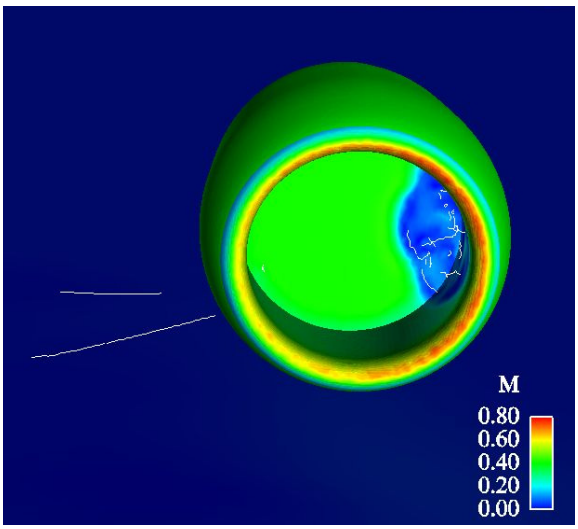


Figure 8 – Mach number isocontours on the nacelle and fan surfaces and vortex cores at 30kts crosswind

The crosswind was subsequently reduced to 5kts and the results are depicted on figure 9: there is no inlet separation and the ground vortex is visible. Mach number on the inlet is close to sonic. The ground is colored by pressure isocountours, where a low pressure region can be seen where the vortex hits it.

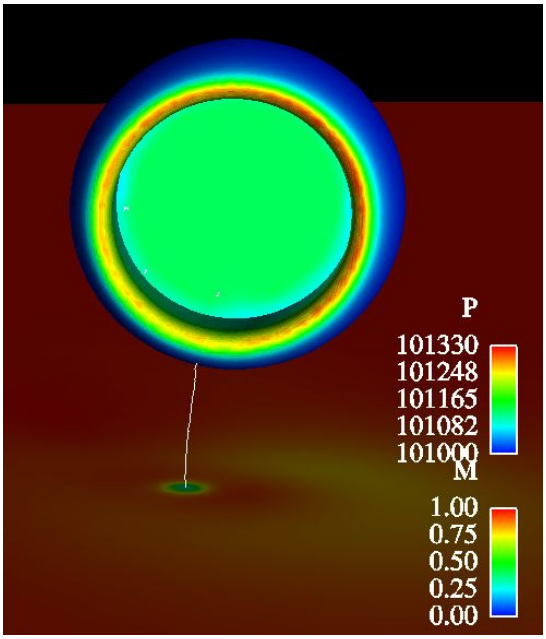


Figure 9 – Mach number isocontours on the nacelle and fan surfaces, vortex cores and static pressure isocountours on the ground at 5 kts crosswind

The vortex detachment from the ground with 15kts cross was unexpected. It was then decided to compare the effects of viscosity on the vortex behavior more directly and cases were run viscous and inviscid at 20kts crosswind, Results for these cases can be seen on fig.10 without and with viscosity respectively. Although both cases exhibit inlet separation the Euler case shows a vortex that does not attach to the ground, the viscous case has a vortex attached to the ground.

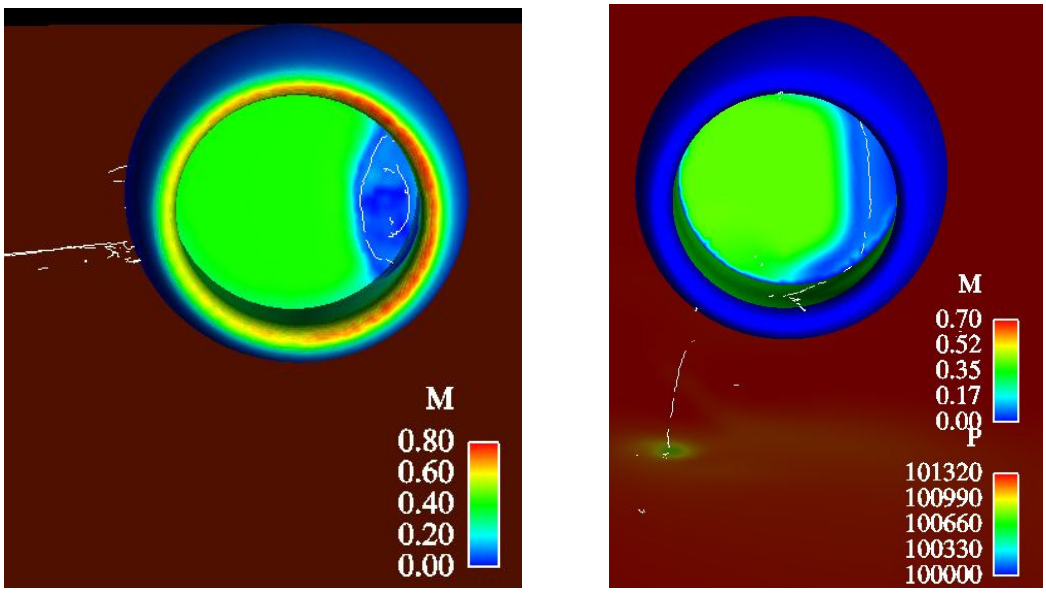


Figure 10 – Mach number isocontours on the nacelle and fan surfaces, vortex cores and static pressure isocontours on the ground at 20 kts crosswind, Euler and Navier-Stokes calculations respectively.

Besides the marked difference on the ground vortex behavior, the separation region has a different shape which can be seen through the lower pressure region on the fan face. It is clear that the viscosity plays an important role on both vortex and separation phenomenon and can not be disregarded.

### 4.3. Lip cross-section

Results of the DLR F6 MOD1 nacelle were compared with results from other applications with similar contraction ratios. At equivalent winds and engine thrust the DLR F6 MOD1 nacelle had inlet separation, while other nacelles did not. It was then clear that other factors influenced separation. Other geometrical parameters where then analyzed, among them the inlet lip leading edge shape: it was modified from a circular leading edge to an elliptical cross section. Results for a 30 kts crosswind for this MOD2 nacelle are shown on Figure 11.

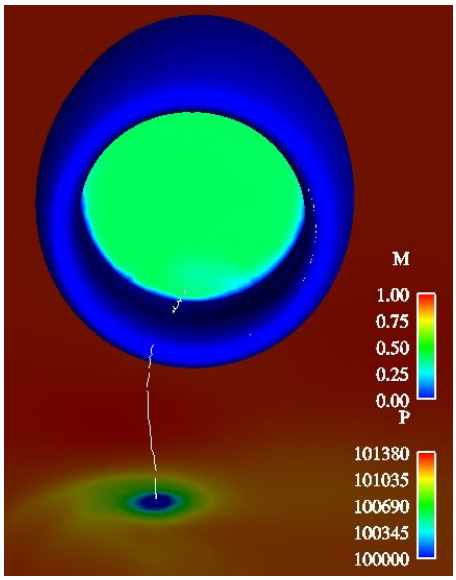


Figure 11 – Mach number isocontours on the MOD2 nacelle and fan surfaces; vortex cores and static pressure isocontours on the ground at 20 kts crosswind.

The fan surface Mach number, on figure 11, indicates that the inlet is not separating anymore; showing that, besides the contraction ratio, the inlet lip geometry also influences inlet separation. Another interesting results, comparing the static pressure on the ground of figures 10 and 11 is that the separated nacelle vortex is less strong than the attached nacelle. This indicates that the highest probability of foreign objects ingestion by the engine is not necessarily with the highest wind intensity if the nacelle inlet lip flow separates at some point.

## 5. Conclusions

Ground vortex visualization still do not have appropriate tools available, none of the methods used was capable of fully detect the vortex. Among the methods tested the vortex core presented the best results.

Comparison between viscous and inviscid calculations showed different results, with the vortex in the inviscid calculation detaching from the ground at a lower crosswind speed and the inlet separation pattern different than the viscous analysis. The vortex phenomena is usually considered to be inviscid, however the interaction of the vortex with the ground shear layer has a viscous effect that needs to be taken into account, when simulating a ground vortex, to represent correctly the phenomena.

In regards to inlet separation, other geometrical parameters than the contract ratio are of influence, the lip cross-section among them. An elliptical lip cross section is less prone to separation than a circular one. Inlet separation also influences on ground vortex strength, a separated inlet vortex is less strong than an attached inlet one. Therefore its possible for a nacelle separated at high crosswinds to be less susceptible to foreign object ingestion than the same nacelle at lower crosswinds with the inlet flow attached.

## 6. References

Beale, D.K., Cramer K.B, King P.S., 2002, "Development of Improved Methods for Simulating Aircraft Inlet Distortion in Turbine Engine Ground Tests", Proceedings of the 22nd AIAA Aerodynamic Measurement Technology and Ground Testing Conference, 24-26 June 2002, Saint Louis, USA. AIAA 2002-3045.

Boles, M. A., Stockmann, N. O., 1979, "Use of Experimental Separation Limits in the Theoretical Design of V/STOL Inlets", Journal of Aircraft, Vol.1, No. 1, pp. 29-34.

Colehour, J.L. , Farquhar, B.W., 1971, "Inlet Vortex", Journal of Aircraft, Vol. 8, No. 1, pp. 39-43.

De Souza, F.J, De Jesus, A.B., 2006, "CFD Study of the Influence of Geometrical Parameters on Nacelle Design", Proceedings of ENCIT 2006, ABCM, Curitiba, Brazil.

DLR F6 Geommetry. 2nd AIAA Drag Prediction Workshop, 2003, http://aaac.larc.nasa.gov/tsab/cfdlarc/aiaa-dpw/Workshop2/DLR-F6-geom.html

Ensight User's Manual for Version 8.0, 2005, Computational Engineering International, Inc., Apex, EUA

Haimes, H., Jordan, K., "A Tractable Approach to Understanding the Results from Large-Scale 3D Transient Simulations", AIAA-2000-0918, Jan. 2001.

Jeong, J., Hussain, F., 1995, "On the identification of a vortex". Journal of Fluid Mechanics, 285, pp. 69-94

Johns , C. J., 2002, "The Aircraft Engine Inlet Vortex Problem", AIAA-2002-5894, 2002.

Nakayama , A., Jones , J.R., Correlation for Formation of Inlet Vortex, AIAA Journal, Vol. 37, No.4, 508-510, 1999.

SAE Aerospace Information Report, Inlet Total-Pressure-Distortion Considerations for Gas-Turbine Engines, AIR1419 Rev. A (1999).

Strawn, R., Kenwright, D., 1999, "Computer Visualization of Vortex Wake Systems", AIAA Journal, Vol. 37, No.4, pp. 511-512.

Sajardoen, A., Post, F.H., Ma, B., Banks, D.C., Pagendarm, H.G., 1998, "Selective Visualization of Vortices in Hydrodynamic Flows", IEEE Visualization, pp: 419-422.

Tourrette, L., 2002, "Navier-Stokes simulations of air-intakes in crosswind using local preconditioning", Proceedings of the 32nd AIAA Fluid Dynamics Conference and Exhibit, 24-26 June 2002, Saint Louis, USA. AIAA 2002-2739.

Yadlin, Y., Shmilovich, A., 2006, "Simulation of Vortex Flows for Airplanes in Ground Operations", Proceedings of the 44th Aerospace Sciences Meeting & Exhibit, 9-12 January, 2006, Reno, NV, USA. AIAA-2006-0056.

## 7. Copyright Notice